

Original article

Digital assessment of gingiva morphological changes and related factors after initial periodontal therapy

Jingran Zhang, Zhen Huang, Yu Cai, and Qingxian Luan

Department of Periodontology, Peking University School and Hospital of Stomatology, Beijing, P. R. China

(Received March 29, 2020; Accepted July 15, 2020)

Abstract

Purpose: To establish a digital assessment method for changes in gingiva morphology following initial periodontal therapy.

Methods: Ten periodontal-healthy participants were selected, and digital models obtained by intraoral scanning and digitizing conventional impressions. Using dentition as a reference, best fit alignment between digital models was carried out. Root mean square (RMS) was calculated to evaluate differences in models, and gingival volume discrepancy (GVD) was calculated after combining separated models. Trueness of intraoral scanning used on the gingiva was evaluated using RMS and GVD between intraoral and conventional models with conventional models as references; precision was evaluated among different intraoral models of one participant. Twenty-three periodontitis-affected participants underwent intraoral scanning immediately after supragingival scaling and two weeks after initial periodontal therapy. The GVD of gingiva between two digital models was calculated to assess gingival changes and related factors after therapy.

Results: Trueness of intraoral scanning used on the entire gingiva was $83.65 \pm 14.43 \mu\text{m}$; precision was $70.71 \pm 25.58 \mu\text{m}$; GVD error measured by digital models was $15.28 \pm 10.00 \text{ mm}^3$. Gingival volume in periodontitis-affected participants decreased $104.04\text{--}1155.09 \text{ mm}^3$ after therapy. Probing depth, bleeding index, and keratinized gingival width positively correlated with changes in gingival volume.

Conclusion: Intraoral scanning can be recommended as a method of evaluating morphological changes in gingiva.

Keywords; digital dentistry, gingival morphology, gingival volume, intraoral scanning, periodontitis

Introduction

Periodontitis, a common oral disease, can lead to morphological changes in the gingiva, manifesting as gingival recession and papilla area “black triangle”. Abundant soft tissue has an important role in preventing the adverse effects of periodontal surgery, restoration, and orthodontic treatment [1,2], and gingival changes after treatment can be seen as a reflection of reduced inflammation [3]. Accordingly, it is important to evaluate changes in soft tissue. Comprehensive examinations of patients were carried out, mostly using periodontal probe and radiographic methods [4], in order to evaluate soft tissue changes before and after treatment. Studies reported that gingival recession was approximately 1.3-1.4 mm 13 months after nonsurgical therapy and at most 1.8 mm in cases of severe advanced periodontitis in non-molar sites [5,6]. Previous methods were two-dimensional, but there is little information on gingival three-dimensional changes in volume or influencing factors.

Intraoral scanning is the basis of digital design and manufacture in dentistry. Studies have confirmed both reliability and validity in use on single teeth and dentition [7-10]. Moreover, it is clinically accurate in

capturing the contour of gingiva near the teeth and palatal mucosa [11-14]. This technology can assess changes in the soft tissue around a single tooth or implant after mucogingival surgery and implantation [14,15]. To the best of the authors’ knowledge, the accuracy (trueness and precision) [16] of intraoral scanning used on the entire gingiva remains unclear. This technology has not been used to assess changes in the gingiva after initial periodontal therapies.

Accordingly, the aim of this study was to propose a digital method of evaluating morphological differences in the gingiva and assessing volumetric changes in gingiva and related factors in patients with periodontitis after initial periodontal therapy.

Materials and Methods

This observational study was approved by the institutional review board of Peking University Hospital of Stomatology (PKUSSIRB-201734046). It was conducted in accordance with the Helsinki Declaration of 1975, as revised in 2013. According to the time sequence and study design, participants in the healthy group (Group H) were initially enrolled, followed by those in the periodontitis group (Group P). The study workflow is shown in Fig. 1.

Group H

Group H comprised 10 periodontal healthy participants. Inclusion criteria were as follows: good oral hygiene with calculus index = 0, no swollen gingiva with bleeding index ≤ 1 , probing depth ≤ 3 mm, continuous dentition except for the third molars, and systemically healthy. Exclusion criteria were crowded dentition, tooth features absent because of erosion, ongoing orthodontic treatment, and smoking. All Group H participants received extensive information about the study, signed an informed consent document, and underwent the following examinations.

Intraoral scanning

All periodontal healthy participants (H1-H10) underwent maxillary and mandibular full-arch dentition and gingiva scanning (SM 1-10) with an intraoral scanner (TRIOS POD 2, 3 Shape Inc., Copenhagen, Denmark) performed by an experienced operator immediately after brushing. The scanning process was conducted according to the manufacturer’s guidelines. Scanning started at the occlusal-palatal surfaces of the right second molar, moved to the other side of the arch and returned from the buccal side [17]. The alveolar mucosa beyond the mucogingival junction was also scanned to ensure the complete capture of keratinized gingiva and teeth. Intraoral scanning images were exported in STL file format.

One of the participants (H1) underwent additional intraoral scanning at nine different times with the same researcher using the same method. A total of 10 maxillary and 10 mandibular scanning digital models (DM 1-10) of H1 were obtained.

Conventional impressions and digitization of stone casts

Maxillary and mandibular vinyl polysiloxane impressions (Silagum Mix-Star Putty Soft, DMG GmbH, Hamburg, Germany) of Group H were taken 10 minutes after intraoral scanning. The impressions were poured with die dental stone (Heraeus Kulzer GmbH, Hanau, Germany) corresponding to the workflow routinely implemented for diagnostic casts under the same conditions. All casts were stored at a temperature of 20-25°C for one week before being scanned using a high-resolution desk reference scanner

Correspondence to Dr. Qingxian Luan, Department of Periodontology, Peking University School of Stomatology, 22 Zhongguancun South Avenue, Beijing 100081, P. R. China

Fax: +86-10-62173402 E-mail: kqluanqx@126.com

J-STAGE Advance Publication: November 20, 2020

Color figures can be viewed in the online issue at J-STAGE.

doi.org/10.2334/josnusd.20-0157

DN/JST.JSTAGE/josnusd/20-0157

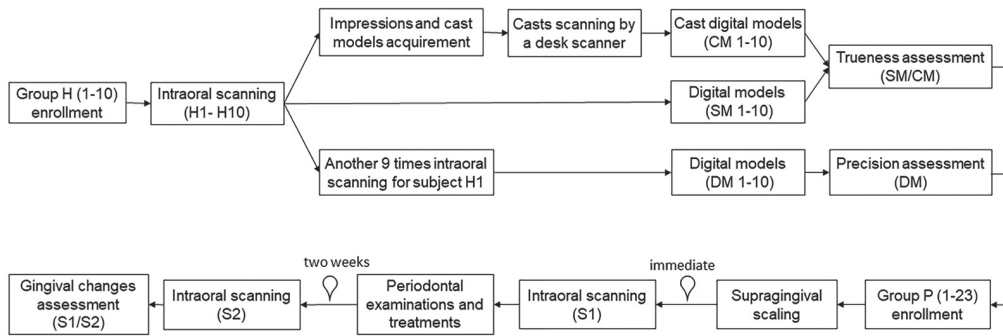


Fig. 1 Workflow of the study design

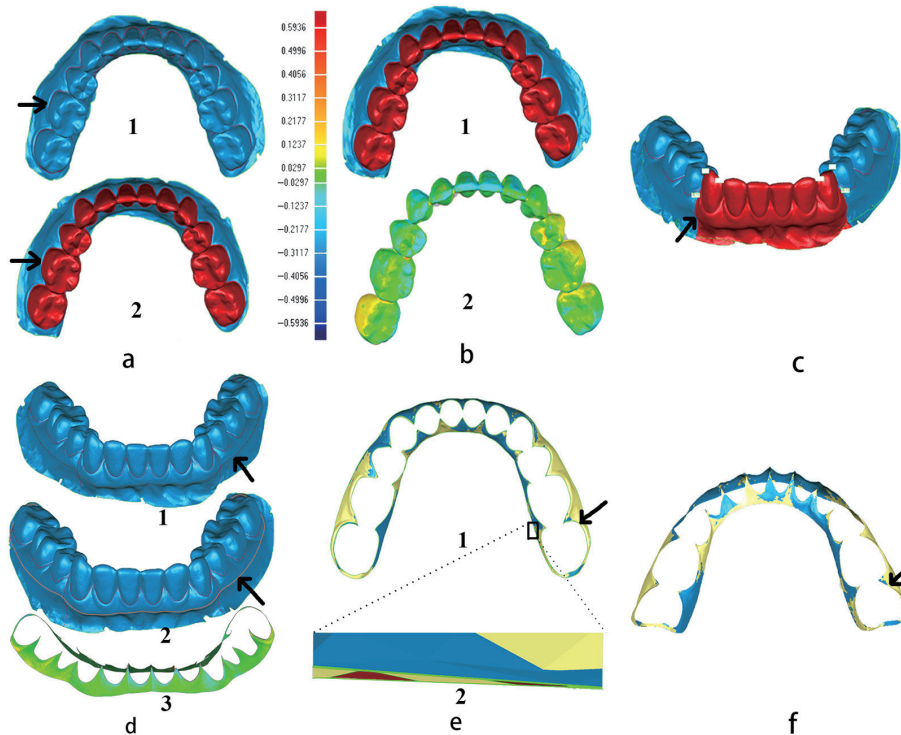


Fig. 2 Management of two compared digital models

a. Creation of gingival margin boundary on the digital models. 1: arrow points to the boundary of the reference model; 2: boundary on the test model; selected areas (teeth) are shown in red, and non-select areas (soft tissue) are shown in blue. b. Best fit alignment of two digital models using the selected whole dentition as a reference. 1: two models after best fit alignment; 2: RMS and color-coded map are calculated to check the alignment. In the spectrum, the closer to the center of the color green, the less the RMS. c. The models are trimmed simultaneously between canines and 1st premolars, and boundaries on cross section can be obtained. Each model is divided into three sections, and every section can be selected alone and aligned. On this alignment, the occlusal surface plus specific buccal and lingual surfaces were selected as references for a more precise alignment. d. Creation of boundaries on the mucogingival junction. Taking two whole models as an example. 1: a curve created by the mucogingival junction on the reference model. 2: projection of the curve to the test model to obtain the same mucogingival junction boundary. 3: RMS and color-coded map of the gingiva are calculated. e. Combination of models. 1: Areas of teeth and soft tissue beyond the mucogingival junction are deleted, normal of the test model is reversed, and the remaining gingiva of the reference and test models are combined to create one model with the original reference model and the original test model as the outer and the inner surfaces, respectively. The combined model is unsealed with the green-colored border (arrow). 2: Magnified selected small area of the outer and the inner surface with unsealed borders. Before the borders are sealed, several bridges are built between the borders (red areas). f. Volume calculation of the combined, sealed model, which is the GVD between the reference and test models.

(DS-EX Pro scanner, Shinning 3D Inc., Hangzhou, P. R. China) with an accuracy of $10\ \mu\text{m}$. The scanner was used according to the manufacturer's instructions to obtain cast digital models (CM 1-10), which were exported as STL files.

Digital model assessment

All digital models were assessed using reverse engineering software (Geomagic studio 12, 3D Systems Inc., Rock Hill, SC, USA).

The accuracy (trueness and precision) of intraoral scanning was assessed by evaluating discrepancies between different models. Trueness was defined in this study as differences of SM from CM, and precision as differences among DMs. Trueness provided information on errors arising as a result of intraoral scanning, whereas precision evaluated repeatability. Accuracy was an overall parameter of combined "trueness" and "precision" [16].

The discrepancy between two digital models was mainly evaluated

using root mean square (RMS). When one model was set as a reference model and the other as a test model, RMS was calculated by averaging the absolute distances of thousands of random points on the model surfaces [18,19] according to the following equation:

$$RMS = \sqrt{\frac{\sum_{i=1}^n (x_{1,i} - x_{2,i})^2}{n}}$$

where $x_{1,i}$ is the point of the reference model, and $x_{2,i}$ is the same point of the test model. The smaller the RMS value, the smaller the difference between the two models and the better the accuracy.

Digital models reflect the surface information of the gingiva and teeth without inner texture. The actual gingival volume cannot be obtained, but gingival volume differences between two models can be calculated. If two digital models share the same dentition, after superimposition using dentition as a reference and removal of dentition and irrelevant mucosa, the

Table 1 Trueness of intraoral scanning (μm)

	<i>n</i>	Range	Mean \pm SD	Test of normality	Test of homoscedasticity	<i>P</i> -value [†]
Den [‡] + Gin [‡]	20	46.00-118.00	86.78 \pm 19.68	0.309		
Den	20	46.00-109.00	79.15 \pm 18.32	0.286	0.481	0.217
Gin	20	56.00-107.00	83.65 \pm 14.43	0.824		
A [‡] Den + A Gin	20	40.00-101.00	69.88 \pm 15.91	0.984		
A Den	20	45.00-88.50	63.72 \pm 14.2	0.087	0.853	0.091
A Gin	20	47.50-103.00	70.13 \pm 14.87	0.553		
P [‡] Den + P Gin	20	34.00-104.00	68.05 \pm 14.96	0.115		
P Den	20	33.50-85.50	60.31 \pm 14.33	0.072	0.730	0.062
P Gin	20	50.00-93.00	66.83 \pm 13.30	0.750		

[†]differences between dentition and gingiva; [‡]Den, dentition; Gin, gingiva; A, anterior; P, posterior

Table 2 Precision of intraoral scanning (μm)

	<i>n</i>	Range	Mean \pm SD	Test of normality	Test of homoscedasticity	<i>P</i> -value [†]
Den [‡] + Gin [‡]	18	33.00-103.70	64.03 \pm 19.33	0.768		
Den	18	40.50-104.70	66.20 \pm 18.68	0.448	0.392	0.130
Gin	18	31.40-125.30	70.71 \pm 25.58	0.787		
A [‡] Den + A Gin	18	25.00-58.20	40.15 \pm 8.86	0.608		
A Den	18	31.00-64.40	43.41 \pm 10.30	0.065	0.525	0.169
A Gin	18	23.30-78.70	38.17 \pm 14.93	0.056		
P [‡] Den + P Gin	18	31.50-138.00	72.97 \pm 27.33	0.518		
P Den	18	27.20-127.80	69.51 \pm 26.32	0.841	0.990	0.034
P Gin	18	32.50-151.00	75.98 \pm 29.60	0.054		

[†]differences between dentition and gingiva; [‡]Den, dentition; Gin, gingiva; A, anterior; P, posterior

space between the remaining gingiva represents the difference in gingival volume. In this study, this was referred as the gingival volume discrepancy (GVD). The GVD among DMs and between SM and CM was an additional examination of the accuracy of intraoral scanning used on the gingiva, showing the error in calculating gingival volume differences using this method. Moreover, GVD was the main parameter used to evaluate gingival volume changes.

The measuring procedure comprised trim and deletion, best fit alignment, and calculation of RMS and GVD. Figure 2 shows the details of management of two digital models. To evaluate the trueness of intraoral scanning, CM and SM were used as the reference model and the test model, respectively. A total of 10 pairs of maxillary and 10 pairs of mandibular models were used. For precision, DM1 and DM 2-10 were set as reference and test models, respectively. Thus, 9 pairs of maxillary and 9 pairs of mandibular models were used. When evaluating separated sextants, areas of interest were selected and others were ignored. Examiner reproducibility of measurements on digital models was assessed using an intraclass correlation coefficient of 0.943.

Analysis of the digital models of Group H showed the accuracy of intraoral scanning used on the entire gingiva, and the error of the method to assess differences in gingival volume between the two digital models.

Group P

Group P comprised 23 participants who were enrolled to assess changes in gingival volume after initial periodontal therapy using the above-described method.

The inclusion criteria were as follows: diagnosis of chronic periodontitis according to the 1999 classification of periodontal diseases and conditions, tooth mobility $\leq 1^\circ$, no periodontal treatment history for at least 6 months, continuous dentition except for 3rd molars, and systemically healthy. The exclusion criteria were the same as those for Group H. The participants received extensive information about the study, signed an informed consent document, and underwent the following examinations and treatments.

Intraoral scanning

All Group P participants underwent intraoral scanning of maxillary and mandibular full dentition and gingiva twice immediately after supragingival scaling (S1) and two weeks after the initial periodontal therapy (S2). The scanner used, the scanning process, and the operator were the same as those for Group H. A total of 23 pairs of maxillary and 23 pairs of mandibular digital models were obtained.

Periodontal examinations and treatments

All Group P patients received supragingival scaling by another well-trained periodontal doctor before the first intraoral scanning. They underwent

thorough periodontal examinations after supragingival scaling including probing depth (PD, 6 sites of distal-buccal, buccal, mesial-buccal, mesial-lingual, lingual, distal-lingual); Mazza bleeding index (BI, 2 sites of buccal and lingual); keratinized gingival width (KW, 2 sites of buccal and lingual); gingival recession (GR, 2 sites of buccal and lingual); and mobility (M). Patients received corresponding subgingival scaling and root planing. All clinical examinations and treatments were performed by the same doctor. The doctor's performance was calibrated against that of an experienced periodontist with a kappa value of 0.897; the resulting intra-examiner kappa value was 0.920.

Calculation of changes in gingival volume

Changes in gingival volume before and after therapy were calculated as the GVD between S1 and S2. Digital models S1 and S2 were set as reference and test models, respectively. Management of digital models was the same as that described for Group H (Fig. 2).

Statistical analysis

Standard information and clinical exam data are presented using descriptive statistics and *t*-testing. Assessments and comparisons of gingival changes were analyzed using repeated measures ANOVA and *t*-test. Normality of the data was analyzed by Shapiro-Wilk test. Homoscedasticity of the data was analyzed by Levene's test. Correlations among different factors were analyzed by bivariate correlation. Analysis was performed with SPSS 24.0 (IBM, Armonk, NY, USA). Differences were considered significant at *P* < 0.05.

Results

Trueness and precision of intraoral scanning in gingiva

Table 1 shows trueness of intraoral scanning in different tissues. Trueness of the entire gingiva was $83.65 \pm 14.43 \mu\text{m}$, and data were normally distributed (*P* = 0.824). Homoscedasticity was found between the data of trueness in gingiva and dentition (*P* = 0.481), and differences between them were not statistically significant with *P* = 0.217. Regardless of whether in anterior or posterior sextants, which were all in a normal distribution (*P* > 0.05), the trueness of gingiva and dentition were homoscedastic (*P* = 0.853 and 0.730, respectively), and no significant differences were observed between them (*P* = 0.091 and 0.062, respectively). However, differences were observed between the whole models and the divided sextants (*P* < 0.05).

The entire GVD between SM and CM was calculated with a mean of $-6.87 \pm 29.35 \text{ mm}^3$ and 95% confidence interval of $-20.60-6.86 \text{ mm}^3$. In this study, CMs were set as reference models and SMs as test models; thus, negative volume differences showed that the CM gingiva was "smaller"

Table 3 Clinical information at baseline in sextants

		Range	Mean \pm SD	(+) %
Anterior	PD [§]	2.30-8.46	4.20 \pm 1.11	37.0 [†]
	BI [¶]	1.00-4.25	3.00 \pm 0.82	
	KW ^{§§}	2.22-7.73	4.79 \pm 1.33	
	PD	2.30-8.46	3.92 \pm 1.29	21.7 [†]
	BI	1.00-4.25	2.85 \pm 0.89	
	KW	2.73-7.27	5.08 \pm 1.32	
Left posterior	mobility			28.0 [‡]
	PD	3.00-8.23	4.38 \pm 1.05	50.0 [†]
	BI	1.13-4.00	3.06 \pm 0.80	
	KW	2.65-7.66	4.58 \pm 1.35	
Right posterior	mobility			10.8 [‡]
	PD	3.00-7.21	4.31 \pm 0.93	43.5 [†]
	BI	1.63-4.00	3.10 \pm 0.77	
	KW	2.22-7.73	4.71 \pm 1.29	
	mobility			4.3 [‡]

[§]PD, probing depth; BI, Mazza bleeding index; KW, keratinized gingival width; [†]the percentage of positive values of difference between PD and KW; [‡]the percentage of teeth with mobility; [¶]unit: mm

Table 4 Changes in gingival volume after initial therapy (mm³)

		Range	Mean \pm SD	Test of normality	Test of homoscedasticity [†]	P-value [‡]
Maxilla	Full jaw	104.04-1155.09	433.43 \pm 227.55			
	Anterior	34.01-423.91	132.96 \pm 88.94	0.055	0.336	0.047
	Left posterior	34.06-444.22	157.41 \pm 91.48	0.051		
	Right posterior	19.55-343.55	141.32 \pm 69.45	0.054		
	Full jaw	104.04-894.31	469.53 \pm 227.40			
	Anterior	37.02-336.57	138.63 \pm 88.07	0.057	0.389	0.055
Mandible	Left posterior	34.06-444.22	178.60 \pm 99.00	0.055		
	Right posterior	19.55-343.55	148.50 \pm 70.48	0.115		
	Full jaw	156.25-1155.09	398.90 \pm 227.25			
	Anterior	34.01-423.91	127.29 \pm 91.42	0.141	0.719	0.618
	Left posterior	39.98-401.33	147.14 \pm 69.31	0.188		
	Right posterior	21.44-329.85	134.46 \pm 69.31	0.066		

[†]differences among anterior, left posterior and right posterior gingiva

Table 5 Correlations between gingival volume changes and other factors

		PD ^{§†}	BI ^{§†}	GR ^{§†}	KW ^{§†}	Age [‡]	Sex [‡]
V [§]	Correlation coefficient	0.833**	0.695**	-0.021	0.426**	-0.183	-0.014
	P-value	<0.001	<0.001	0.889	0.004	0.228	0.929
	n	46	46	46	46	46	46

[§]PD, probing depth; BI, Mazza bleeding index; GR, gingival recession; KW, keratinized gingival width; V, gingival volume changes of a single jaw; [†]PD, GR and KW followed a normal distribution, Pearson's correlation was applied; [‡]BI and sex are rank data, and the distribution of age was not normal, Spearman's correlation was applied; **correlation is significant at the 0.01 level (2-tailed)

than the SM gingiva. Large discrepancies were found in the posterior area.

Assessment of precision of intraoral scanning is shown in Table 2. Similar to trueness, the data of gingiva and dentition were normally distributed with $P > 0.05$, and were homoscedastic with $P = 0.392$ in the entire gingiva and dentition, 0.525 in anterior region, and 0.990 in posterior region. The precision of the entire gingiva and dentition was also comparable, with $P = 0.130$. A difference was observed between posterior dentition and gingiva ($P = 0.034$), with a mean difference of $-6.47 \mu\text{m}$. Anterior sextants had the smallest RMS with $P < 0.05$, whereas posterior sextants were larger.

The entire GVD among DMs was $15.28 \pm 10.00 \text{ mm}^3$, with a 95% confidence interval of 10.30-20.25 mm³. DM1 was set as a reference model for comparison with DM 2-10. Thus, differences were accepted as absolute values to evaluate the mean differences among them. Using this method to measure the entire gingival volume differences between the two models means that the error can be accepted as 15.28 mm³.

The above results confirmed the trueness and precision of intraoral scanning used in the entire gingiva and calculation of the GVD.

Group P participants

The final population meeting the study criteria comprised 23 periodontitis-affected participants aged 25-53 years, with a mean age of 32 ± 6.89 years. Males and females were almost equally represented, with 11 males and 12 females included. All were systemically healthy and non-smokers. All patients received subgingival scaling and root planing.

Clinical assessment of Group P

Most participants in Group P suffered mild to moderate periodontitis with a mean PD of ≤ 6 mm. Only 1 participant had a mean PD more than 6 mm but no more than 8 mm; 11 participants had a mean PD of 4-6 mm, and for the other 11 participants it was no more than 4 mm. In approximately 37% of sextants, the mean PD was greater than KW. PD, KW and GR all followed normal distributions with $P = 0.200$, 0.231 and 0.065, respectively. Two participants had a mean BI less than 2, and the others all bled on probing with a mean BI of 3. No tooth had mobility more than I°. Males and females had similar clinical situations and no statistical difference was observed between them. Table 3 shows baseline clinical information of the participants.

Changes in gingival volume of Group P

Changes in the entire gingival volume after initial periodontal therapy in a single jaw were 104.04-1155.09 mm³, with a mean of $433.43 \pm 227.55 \text{ mm}^3$ according to different participants. The error of 15.28 mm³ accounted for 3.52%. Whether it was in a single jaw or different sextants, the changes in gingival volume were all normally distributed with $P > 0.05$. Changes in different sextants were homoscedastic with $P > 0.05$, and the anterior gingiva changed less than the posterior gingiva ($P = 0.047$) (Table 4). In mild periodontitis with PD ≤ 4 mm, changes in entire volume were $294.42 \pm 76.51 \text{ mm}^3$ in the maxilla and $250.40 \pm 26.48 \text{ mm}^3$ in the mandible. No statistical difference was observed between the maxilla and mandible ($P > 0.05$) in the full jaw or separated sextants. Along with the increase in PD,

in moderate periodontitis with PD 4–6 mm, volume changes increased to $591.60 \pm 198.99 \text{ mm}^3$ in the maxilla and $485.46 \pm 121.80 \text{ mm}^3$ in the mandible. The maxillary gingiva changed more than the mandibular gingiva in posterior sextants with $P < 0.05$.

PD was strongly correlated with changes in gingival volume ($r = 0.833$); KW ($r = 0.426$) and BI ($r = 0.695$) had a moderate correlation. GR ($P = 0.889$), age ($P = 0.228$), and sex ($P = 0.929$) were not correlated with volume changes (Table 5).

Discussion

This study proposed a digital method to evaluate morphological changes in the gingiva, and obtained three-dimensional gingival alterations after initial therapy by comparing different intraoral scanning digital models.

The trueness of an intraoral scanner is the difference between digital models captured by the scanner and the real condition of the oral cavity; however, obtaining direct three-dimensional data of the oral cavity is impossible. An alternative method was adopted using vinyl polysiloxane impression and die dental stone in this study. The accuracy of the combination was confirmed by clinical and scientific research. Addition silicone impression was considered as the standard impression material [8,20]. Despite errors in impression, cast models, and model scanning, the combination of vinyl polysiloxane impression and cast model scanning has been employed in numerous studies to evaluate intraoral scanning accuracy [19,21,22].

To evaluate the difference between two digital models of one participant, best fit alignment was applied before calculating the RMS. Best fit alignment uses an iterative closest point algorithm to search for the best matching location between data sets, and does not depend on operator-based decisions. According to the nature of the iterative closest point, alignment is performed by minimizing the mesh distance error between each corresponding data point. This operation evenly distributes the error on the positive and negative deviations [18]. If discrepancies exist between models, the algorithm attempts to minimize the absolute distance between the two datasets, regardless of the clinical outcome. This may explain the negative value on the calculation of GVD between models by selecting the outer and inner surfaces manually.

To overcome the above error, previous studies attempted to align surface areas that experienced changes below a predefined threshold instead of entire models. These areas were seen as an align reference and the method was reported to be superior [23]. O'Toole et al. compared the accuracy of "reference best fit alignment", "best fit alignment", and "landmark-based alignment". A reference model was digitally manipulated to remove specific areas, randomly repositioned to get the test model, and then the two models were aligned using different alignment strategies. Reference best fit alignment produced significantly lower alignment errors and truer measurements [18]. Thus, the greatest challenge in aligning digital models of different models or different time points is to identify a stable structure that can be used as a reference [24]. Teeth could be used as such a reference given the lack of mobility in Group H, and mobility less than 1° before and after treatments in Group P [25,26]. The accuracy of intraoral scanning used on teeth has been previously established [27–29]. According to the various scanners and methods applied, the trueness and precision of dentition scanning were $17\text{--}378 \mu\text{m}$ and $55\text{--}116 \mu\text{m}$, respectively, and no significant difference was observed among the scanners [29]. The trueness of $79.15 \pm 18.32 \mu\text{m}$ and precision of $66.20 \pm 18.68 \mu\text{m}$ in dentition obtained in this study (Tables 1 and 2) were consistent with previous studies [27,29], and were applied to evaluate the gingival condition.

For intraoral scanning used on the entire gingiva, trueness was $83.65 \pm 14.43 \mu\text{m}$, and precision $70.71 \pm 25.58 \mu\text{m}$. No statistically significant difference was observed between dentition and gingiva, indicating that intraoral scanning could capture hard and soft tissues at a comparable level. Previous studies on soft tissue accuracy only focused on the palatal mucosa or a limited gingival area adjacent to the marginal gingiva, and the results mostly ranged from 80 to $130 \mu\text{m}$ [11–14,22]. This study confirmed the accuracy of intraoral scanning applied to a larger area of the gingiva.

Compared with SM, CM was a little "smaller" in gingival volume. In the conventional impression procedure, the soft tissue was inevitably compressed by the impression material, causing local deformation. Since the intraoral scanner had no contact with the soft tissue, the above limitation

was avoided. This is more critical when a periodontitis-affected gingiva impression is taken because of the softer and more vulnerable texture of the inflamed gingiva than the healthy gingiva. Conventional impressions may cause more compressions or injuries than intraoral scanning.

Whole dentition and gingiva showed less trueness than divided sextants. Among the sextants, posterior sextants showed less precision than anterior sextants, indicating that in full dentin intraoral scanning, errors may arise more frequently in the posterior area. Studies have shown that with the expansion of the scanning area, scanning errors multiplied [30,31]. In full dentition scanning, the terminal dentition had the largest error. Capturing digital images of molars was more difficult because of complicated contours, existence of the tongue and saliva, and issues with the scanner sensor reaching into the mouth. When superimposing digital models, selecting a limited area of interest before best fit alignment helps to offset scanning errors. Alignment of the entire model may reduce the best fit alignment quality in the focused area.

Although the current accuracy was obtained from participants with healthy gingiva, studies carried out by Zhang et al. [32] confirmed the accuracy of a TRIOS intraoral scanner used on periodontitis-affected participants. Conventional impressions of periodontitis-affected participants were digitized by a reference desk scanner and superimposed to digital models captured by a TRIOS intraoral scanner. A 3 mm-wide region of the gingiva was selected and results showed that the RMS between the two digital models did not correlate with either pocket probing depth or degree of gingival inflammation. Thus, intraoral scanning digital models of periodontitis were clinically applicable.

Changes in the entire gingival volume ranged from 104.04 to 1155.09 mm^3 in a single jaw. PD and BI both showed strong correlation with changes in gingival volume; gingival volume decreased more with the increase in PD and BI. This confirmed that the more severe the gingival inflammation, the more changes occur after periodontal therapies [5,6,33]. Apart from PD and BI, KW was positively correlated with volume changes, indicating that in participants with more keratinized gingiva, more changes in gingival volume can be observed. As the width of keratinized gingiva reflects the position of the mucogingival junction, the result indicated that even in mild periodontitis, inflammation can affect soft tissue beyond the mucogingival junction, particularly in sextants with greater PD than KW, which accounted for approximately 37.0% of all sextants. The mucogingival junction remains stable even if the gingiva is apically repositioned [34], and using it as an alignment reference has been confirmed to be reliable [35]. The current result showed that "stable" means a relative constant position in the coronal-apical direction, rather than in the buccal-lingual direction.

This study focused on three-dimensional assessment of the entire gingiva using intraoral scanning and related digital approaches, and confirmed the trueness and precision of intraoral scanning used on the larger area of soft tissue. Changes in periodontitis gingival volume before and after the initial therapy and related factors were assessed using digital models. The approaches were non-invasive, patient-friendly, and convenient since they compared different digital models at different time points. Differences among digital models revealed changes in gingiva and monitored treatment outcomes, expanding the indicators of clinical efficacy.

This study also had limitations. First, the sample size was small, and the observation period was relatively short. Second, no post-treatment clinical examinations were performed and changes in gingival volume in response to treatment could not be associated with changes in the clinical indices. Third, most periodontitis-affected participants had mild to moderate conditions; therefore, fewer results for severe periodontitis were obtained. Further studies combined with other digital approaches and clinical methods are needed.

In conclusion, after initial periodontal therapy, morphological changes in the gingiva were related to probing depth, bleeding index, and keratinized gingival width. Intraoral digital scanning can be recommended as a method to evaluate morphological changes in gingiva.

Acknowledgments

This work was supported by the Program for New Clinical Techniques and Therapies of Peking University School and Hospital of Stomatology.

Conflict of interest

The authors declare no conflicts of interest.

References

- Zweers J, Thomas RZ, Slot DE, Weisgold AS, Van der Weijden FG (2014) Characteristics of periodontal biotype, its dimensions, associations and prevalence: a systematic review. *J Clin Periodontol* 41, 958-971.
- Gurlek O, Sonmez S, Guneri P, Nizam N (2018) A novel soft tissue thickness measuring method using cone beam computed tomography. *J Esthet Restor Dent* 30, 516-522.
- Mayer Y, Ginesin O, Machtei EE (2017) Photometric CIELAB analysis of the gingiva: a novel approach to assess response to periodontal therapy. *J Periodontol* 88, 854-859.
- Adriaens PA, Adriaens LM (2004) Effects of nonsurgical periodontal therapy on hard and soft tissues. *Periodontol* 2000 36, 121-145.
- Badersten A, Nilveus R, Egelberg J (1981) Effect of nonsurgical periodontal therapy. I. moderately advanced periodontitis. *J Clin Periodontol* 8, 57-72.
- Badersten A, Nilveus R, Egelberg J (1984) Effect of nonsurgical periodontal therapy. II. severely advanced periodontitis. *J Clin Periodontol* 11, 63-76.
- Aragón MLC, Pontes LF, Bichara LM, Flores-Mir C, Normando D (2016) Validity and reliability of intraoral scanners compared to conventional gypsum models measurements: a systematic review. *Eur J Orthodont* 38, 429-434.
- Sason GK, Mistry G, Tabassum R, Shetty O (2018) A comparative evaluation of intraoral and extraoral digital impressions: an in vivo study. *J Indian Prosthodont Soc* 18, 108-116.
- Kihara H, Hatakeyama W, Komine F, Takafuji K, Takahashi T, Yokota J et al. (2019) Accuracy and practicality of intraoral scanner in dentistry: a literature review. *J Prosthodont Res* 64,109-113.
- Medina-Sotomayor P, Pascual-Moscardo A, Camps AI (2019) Accuracy of 4 digital scanning systems on prepared teeth digitally isolated from a complete dental arch. *J Prosthet Dent* 121, 811-820.
- Strebel J, Ender A, Paqué F, Krähenmann M, Attin T, Schmidlin PR (2009) In vivo validation of a three-dimensional optical method to document volumetric soft tissue changes of the interdental papilla. *J Periodontol* 80, 56-61.
- Yan S, Shi SG, Niu ZY, Pei ZH, Shi SM, Mu C (2014) Soft tissue image reconstruction using cone-beam computed tomography combined with laser scanning: a novel method to evaluate the masticatory mucosa. *Oral Surg Oral Med Oral Pathol Oral Radiol* 118, 725-731.
- Deferm JT, Schreurs R, Baan F, Bruggink R, Merckx MAW, Xi T et al. (2018) Validation of 3D documentation of palatal soft tissue shape, color, and irregularity with intraoral scanning. *Clin Oral Investig* 22, 1303-1309.
- Rojo E, Stroppa G, Sanz-Martin I, Gonzalez-Martin O, Alemany AS, Nart J (2018) Soft tissue volume gain around dental implants using autogenous subepithelial connective tissue grafts harvested from the lateral palate or tuberosity area. A randomized controlled clinical study. *J Clin Periodontol* 45, 495-503.
- Tian J, Wei D, Zhao Y, Di P, Jiang X, Lin Y (2019) Labial soft tissue contour dynamics following immediate implants and immediate provisionalization of single maxillary incisors: a 1-year prospective study. *Clin Implant Dent Relat Res* 21, 492-502.
- International Organization for Standardization (1994) Accuracy (trueness and precision) of measurement methods and results — part 1: general principles and definitions. ISO 5725-1, Geneva.
- Müller P, Ender A, Joda T, Katsoulis J (2016) Impact of digital intraoral scan strategies on the impression accuracy using the TRIOS Pod scanner. *Quintessence Int* 47, 343-349.
- O'Toole S, Osnes C, Bartlett D, Keeling A (2019) Investigation into the accuracy and measurement methods of sequential 3D dental scan alignment. *Dent Mater* 35, 495-500.
- Abduo J (2019) Accuracy of casts produced from conventional and digital workflows: a qualitative and quantitative analyses. *J Adv Prosthodont* 11, 138-146.
- Shah S, Sundaram G, Bartlett D, Sherriff M (2004) The use of a 3D laser scanner using superimpositional software to assess the accuracy of impression techniques. *J Dent* 32, 653-658.
- Chen SY, Liang WM, Chen FN (2004) Factors affecting the accuracy of elastometric impression materials. *J Dent* 32, 603-609.
- Gan N, Xiong Y, Jiao T (2016) Accuracy of intraoral digital impressions for whole upper jaws, including full dentitions and palatal soft tissues. *PLoS One* 11, e0158800.
- Tantbirojn D, Pintado MR, Versluis A, Dunn C, Delong R (2012) Quantitative analysis of tooth surface loss associated with gastroesophageal reflux disease: a longitudinal clinical study. *J Am Dent Assoc* 143, 278-285.
- Ioshida M, Munoz BA, Rios H, Cevidanes L, Aristizabal JF, Rey D et al. (2019) Accuracy and reliability of mandibular digital model registration with use of the mucogingival junction as the reference. *Oral Surg Oral Med Oral Pathol Oral Radiol* 127, 351-360.
- Towfighi PP, Brunsvold MA, Storey AT, Arnold RM, Willman DE, McMahan CA (1997) Pathologic migration of anterior teeth in patients with moderate to severe periodontitis. *J Periodontol* 68, 967-972.
- Gaumet PE, Brunsvold MI, McMahan CA (1999) Spontaneous repositioning of pathologically migrated teeth. *J Periodontol* 70, 1177-1184.
- Mangano FG, Veronesi G, Hauschild U, Mijiritsky E, Mangano C (2016) Trueness and precision of four intraoral scanners in oral implantology: a comparative in vitro study. *PLoS One* 11, e0163107.
- Treesh JC, Liacouras PC, Taft RM, Brooks DI, Raiciulescu S, Ellert DO et al. (2018) Complete-arch accuracy of intraoral scanners. *J Prosthet Dent* 120, 382-388.
- Bohner L, Gamba DD, Hanisch M, Marcio BS, Tortamano Neto P, Lagana DC et al. (2019) Accuracy of digital technologies for the scanning of facial, skeletal, and intraoral tissues: a systematic review. *J Prosthet Dent* 121, 246-251.
- Yuzbasioglu E, Kurt H, Turunc R, Bilir H (2014) Comparison of digital and conventional impression techniques: evaluation of patients' perception, treatment comfort, effectiveness and clinical outcomes. *BMC Oral Health* 14, 10.
- Guth JF, Runkel C, Beuer F, Stimmelmayer M, Edelhoff D, Keul C (2017) Accuracy of five intraoral scanners compared to indirect digitalization. *Clin Oral Investig* 21, 1445-1455.
- Zhang X, Wu J, Ren S, Yang J, Miao L, Sun W (2018) Study on precision of application of intraoral scanning digitized model into evaluation on region of gingival parenchyma in patients with chronic periodontitis. *Stomatology* 38, 422-427.
- Nordland P, Garrett S, Kiger R, Vanooteghem R, Hutchens LH, Egelberg J (1987) The effect of plaque control and root debridement in molar teeth. *J Clin Periodontol* 14, 231-236.
- Ainamo A, Bergenholtz A, Hugoson A, Ainamo J (1992) Location of the mucogingival junction 18 years after apically repositioned flap surgery. *J Clin Periodontol* 19, 49-52.
- Ioshida M, Muñoz BA, Rios H, Cevidanes L, Aristizabal JF, Rey D et al. (2019) Accuracy and reliability of mandibular digital model registration with use of the mucogingival junction as the reference. *Oral Surg Oral Med Oral Pathol Oral Radiol* 127, 351-360.